DOI: 10.26599/FSHW.2025.9250890

Contents lists available at SciOpen

Food Science and Human Wellness

journal homepage: https://www.sciopen.com/journal/2097-0765

China Food Publishing Co.

Sandwich-Type SERS Aptasensor Based on Aptamer-functionalized Magnetic Capture Probe and AuNPs@MIL-101 Signal Enhancement Probe for Ultrasensitive Detection of *Bifidobacterium bifidum*

Huan Li[a], Zhuangzhuang Tang[a], Jian Chen[a], Qianwei Fan[c], Huiqun Xu[c], Song Miao[d], Yanbo Wang[b,*]

[a]*Food Safety Key Laboratory of Zhejiang Province, School of Food Science and Biotechnology, Zhejiang Gongshang University, Hangzhou, 310018, P. R. China*

[b]*School of Food and Health, Beijing Technology and Business University, Beijing, 100048, P. R. China*

[c]*Wuyi County Inspection and Testing Research Institute, Wuyi, 321200, P. R. China*

[d]*Department of Food Chemistry and Technology, Teagasc Food Research Centre, Moorepark, Ireland*

ABSTRACT: Rapid and on-site detection of *Bifidobacterium bifidum (B. bifidum)* throughout the food manufacturing process serves as an essential sentinel for assessing product quality and healthy potency. Herein, we introduce a sandwich-type surface-enhanced Raman scattering (SERS) aptasensor for *B. bifidum* quantification, which integrates aptamer-functionalized magnetic beads (Apt-Fe_3O_4) for target-specific capture and aptamer-modified gold nanoparticles/metal-organic framework composites (Apt-AuNPs@MIL-101) for SERS-based signal amplification. Experimental results revealed a strong linear correlation between the intensity of the characteristic Raman peak and the logarithmic of the *B. bifidum* concentrations within the range of 2.0×10^1 to 2.0×10^6 CFU/mL, and the limit of detection was as low as 2.5 CFU/mL. In addition to superior sensitivity, the proposed approach demonstrated exceptional specificity against non-target bacterial strains, particularly in multi-strain coexistent systems. The method further demonstrated great potential in analysis of *B. bifidum* in commercial samples, showing high consistency with the results obtained from the classic qPCR method. The study established an innovative analytical platform for rapid and on-site probiotic assessment, highlighting its applicability in probiotic food products' quality control and evaluation.

Keywords: probiotic; SERS; aptamer; magnetic beads; nanocomposites; *Bifidobacterium bifidum*

1. Introduction

Bifidobacterium bifidum (B. bifidum) is a probiotic bacterium belonging to the genus *Bifidobacterium*, which is commonly found in mammals' intestinal tract [1]. As a typical member of intestinal microbiota, it is involved in the production of short-chain fatty acids, thereby regulating intestinal pH, inhibiting the colonization of pathogenic bacteria, and enhancing host immune barrier function [1–3]. At the same time, as one of the main microorganisms in breast milk, *B. bifidum* is one of the earliest microbes to colonize in the infants'

***Corresponding author**
Yanbo Wang, Email: wyb1225@163.com

Received 24 April 2025
Received in revised from 25 May 2025
Accepted 27 October 2025

intestinal tract, benefiting the relief of the infant eczema and regulation of the innate immunity [4]. *B. bifidum* has already been certified by the European Food Safety Authority for Quality and Safety (QPS). It often functions in probiotic products such as fermented dairy products, infant milk powder, and dietary supplements [4,5]. During food production, *B. bifidum* contributes to flavor development through the generation of short-chain fatty acids that impart a distinctive sour and refreshing taste. Concurrently, it synthesizes a variety of vitamins and phenolic compounds, thereby creating a unique aroma [6,7]. *B. bifidum* can compensate for the inherent low acid resistance of lactic acid bacteria to improve survival rate in fermented foods, while simultaneously producing various metabolites to exert functional properties [8]. Rapid and on-site detection of the probiotic such as *B. bifidum* can benefit the quality control of probiotic products while deepen the understanding of their health potency [9]. Despite the expanding commercial applications of *B. bifidum* products, a critical technological gap persists in developing rapid and on-site quantitative detection methods for this specific bacterium.

The conventional biochemical culture method remains the gold-standard for the detection of *B. bifidum*. However, it typically takes about 3 days to obtain the results and the operation is relatively cumbersome [10]. Non-culturing alternatives such as quantitative real-time polymerase chain reaction (qPCR) and quartz crystal microbalance methods have been developed for the quantitative detection of *B. bifidum*. The qPCR method detects *B. bifidum* by amplifying the specific gene fragments and using fluorescent signals to quantify the copy number of DNA in real time, which takes a short detection time of 2-4 h and has the characteristics of high specificity and sensitivity. However, its operation is relatively cumbersome, and the consumed reagent is expensive [11]. Quartz crystal microbalances quantify the resonance frequency of quartz crystals by measuring the mass change caused by the target bacteria to the surface of the sensor, which can analyze the number of cells in a sample *in situ* without labeling. It is simple to operate, but lacks sensitivity and is vulnerable to interference from complex matrices [12]. These technical constraints collectively highlight the critical need for developing rapid and on-site detection methods for *B. bifidum*.

Surface-enhanced Raman scattering (SERS) is a rapid spectroscopic technique that is broadly applied in food quality and safety evaluation due to the notable high sensitivity, the ability to provide fingerprint recognition, and on-site detection capability when integrated with a portable instrument [13]. However, the SERS detection methods relied on traditional substrates (e.g., single metal nanoparticles) suffer from the issues of poor signal stability and uneven distribution of hot spots. In this sense, the composite particle system of noble metal nanoparticles/metal-organic framework materials (MOFs) has emerged as novel SERS-active substrates over the past years. The ordered porous framework of MOFs in these composite systems offer stable support for the SERS-active noble metal nanoparticles, forming uniformly distributed hot spots, significantly enhancing the detection sensitivity and reproducibility [14]. With chromium-based MOF MIL-101 (Cr)/noble metal nanoparticles being a notable example, the three-dimensional structure formed by Cr^{3+} and carboxylic acid ligands in MIL-101 (Cr) provided a high-density binding sites for the loading of the noble metal nanoparticles [15]. Li et al. [16] developed MIL-101 (Cr)/gold nanoparticles (AuNPs) by *in-situ*

growth of the AuNPs on the MIL-101 (Cr), thereby generating uniformly distributed hot spots on the surface of MIL-101 (Cr). The composite was used for SERS analysis of the 2-mercaptobenzimidazole, with a limit of detection being 10 $ng \cdot mL^{-1}$. The MIL-101 (Cr)/silver nanoparticles (AgNPs) studied by Zhao et al. [17] demonstrated their efficacy in the detection of malachite green. The confined growth strategy of the AgNPs on the MIL-101 (Cr) framework resulted in the formation of a high-density, homogeneous NP array on its surface. The obtained SERS substrate enabled the ultra-sensitive detection of malachite green with promising signal stability. However, the exploration of such composite SERSs substrates in the rapid and on-site detection of probiotics such as *B. bifidum* is still limited. Moreover, with current SERS sensing methods, detecting target analytes in complex food matrices typically necessitates elaborate data analysis such as deep learning-assisted spectra interpretation [18], or requires coupling with high-cost nucleic acid analysis methods like clustered regularly interspaced short palindromic repeats (CRISPR) techniques [19]. These requirements substantially limit their application in actual detection scenarios. Intergrating with a simple and economical pretreatment method to achieve specific separation of target analyte could be an efficient way to avoid interference from complex food matrices. Among the various separation methods, aptamer (Apt) modified magnetic bead-based separation is believed to be a promising way. For instance, Wang et al. [20] grafted Apt onto the surfaces of gold nanoparticles@macroporous magnetic silica photonic microsphere, which could capture target *Escherichia coli* O157: H7 to enable selective and rapid detection of the target bacteria in small volume sample. To the best of our knowledge, the integration of magnetic separation technology with composite noble metal nanoparticles/MOFs SERS substrates for rapid and on-site detection of probiotics remains relatively underexplored.

In this work, a novel SERS detection system was developed using the Apt functionalized AuNPs@MIL-101 as a signal enhancement probe. It was prepared by grafting Apt after *in-situ* growth of the AuNPs on MIL-101 (Cr). Moreover, an Apt-functionalized Fe_3O_4 magnetic capture probe was incorporated to enable selective and rapid isolation of *B. bifidum* (Scheme 1). After the optimization of key parameters, a sandwich SERS detection platform was constructed and its specificity over nontarget probiotics was analyzed. Also, the pretreatment conditions were explored to achieve reliable detection of *B. bifidum* in commercially available probiotic foods. The detection results were compared with qPCR to verify its accuracy. This study provided a reliable tool for the on-site and rapid detection of the *B. bifidum* in foods.

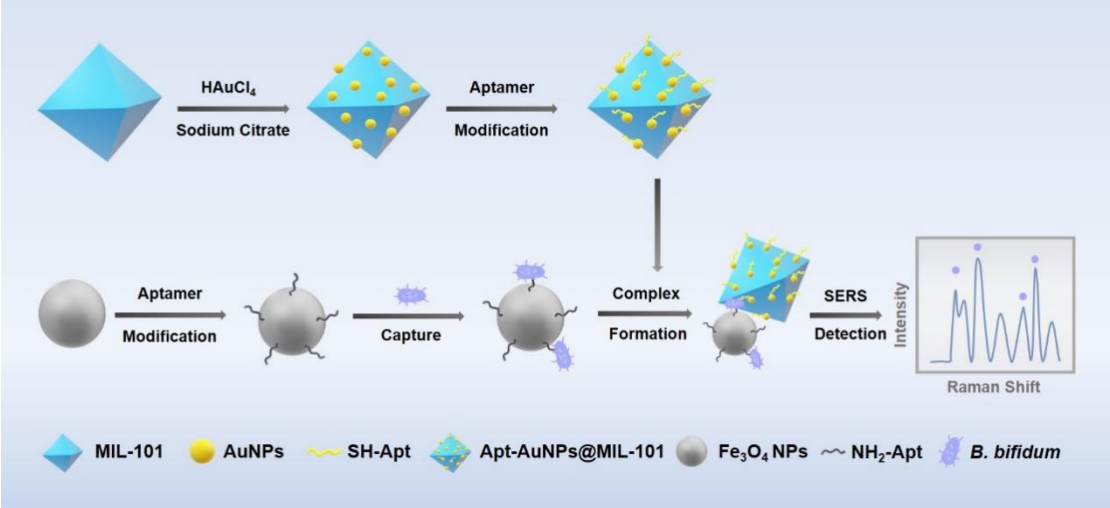

Scheme 1. Schematic diagram of the detection of *B. bifidum* using the sandwich SERS assay based on Apt-Fe_3O_4 capture probe and Apt-AuNPs@MIL-101 MOF signal enhancement probe.

2. Experimental Section

2.1. Materials and Reagents

MIL-101 (Cr) was purchased from Frontier Nano Materials Technology Co., Ltd. (Nanjing, China). Fe_3O_4 magnetic beads, chloroauric acid ($HAuCl_4 \cdot 4H_2O$, 99.9%), sodium borohydride ($NaBH_4$), N-hydroxysulfosuccinimide (NHS, 98%), trisodium citrate ($C_6H_5Na_3O_7 \cdot 2H_2O$, 99.0%), 1-(3-dimethylaminopropyl)-3-ethylcarbodiimide hydrochloride (EDC, 98.5%) were purchased from Aladdin (Shanghai, China). Mupirocin lithium salt and cysteine hydrochloride modified *Lactobacillus delbergii* medium (MRS), 5% cysteine hydrochloride solution were purchased from Haibo Company (Qingdao, China). The strains used in this experiment were all from the Institute of Microbiology of the Chinese Academy of Sciences, which were *B. bifidum* (TS349566), *Bifidobacterium breve* (*B. breve*, ATCC 15700), *Bifidobacterium longum* (*B. longum*, ATCC 15707), *Lactobacillus johnsonii* (*L. johnsonii*, ATCC 43121), *Lactobacillus acidophilus* (*L. acidophilus*, ATCC 4796), and *Lactobacillus casei* (*L. casei*, CICC 23184). The Apt adopted from the previously reported work [21] with the sequences of 3'-SH-AGCAGCACAGAGGTCAGATGTGCGTGAGCGGTAGCCCCGTACGACCCACTGTGGTTGGGCCCTATGCGTGCTACCGTGAA-5' and 3'-AGCAGCACAGAGGTCAGATGTGCGTGAGCGGTAGCCCCGTACGACCCACTGTGGTTGGGCCCTATGCGTGCTACCGTGAA-NH_2-5', qPCR primers (Bbif-tF: GTCAGGTGGGTGTCCCGCGT; Bbif-tR: ATGCCGACGATCTCGACCGG), and phosphate-buffered saline (PBS) were purchased from Sangon Bioengineering Co., Ltd. (Shanghai, China). The baking powder and pure milk used in the experiment were purchased from an online shopping hall in Taobao (China). Milli-Q water (prepared from Millipore, Massachusetts, USA) was used to conduct the experiments.

2.2. Instrument

Morphology and elemental composition were observed using a FEI Tecnai F20 transmission electron microscope (TEM, JEOL JEM-1400Flash, Japan). X-ray diffraction (XRD) analysis was performed on an

X'Pert PRO MPD diffractometer (Netherlands). Scanning electron microscopy (SEM) images were obtained using the field-emission scanning electron microscope (ZEISS Gemini SEM 500, Germany). X-ray photoelectron spectra (XPS) was obtained using a Thermo Scientific K-Alpha spectrometer (Thermo Scientific, UK). Zeta potential and hydrodynamic sizes were determined using a Malvern Zetasizer Nano ZS600 (Malvern, Worcestershire, UK). Portable Raman spectrometer (RMS1000 of Oceanhood Opto-electronics Technology, Shanghai, China) was used to collect Raman spectra.

2.3. Synthesis of the Apt-AuNPs@MIL-101 signal enhancement probe

AuNPs@MIL-101 was synthesized via the previously reported *in-situ* growth method [22]. 50 mg of MIL-101 (Cr) was added in 70 mL Milli-Q water under 10 min vigorous ultrasonication. Then it was heated until boiling. Under strring, 3 mL 1% $HAuCl_4$ was added dropwisely. After 10-min boiling, 220 μL of 10% (w/v) $C_6H_5Na_3O_7 \cdot 2H_2O$ was rapidly added and subsequently stirred for 15 min. The resulting AuNPs@MIL-101 nanocomposites were washed by centrifugation (10,000 r/min, 10 min, two times), and the precipitates were vacuum-dried at 80 ℃. For Apt functionalization, 0.5 mg of AuNPs@MIL-101 was added in 1 mL water and mixed with 10 μL of 5 μmol/L SH-Apt. Then it was incubated at 37 ℃ overnight. Excess Apt was removed via centrifugation (8000 r/min, 5 min).

2.4. Synthesis of the Apt-Fe3O4 capture probe

Apt-Fe_3O_4 probe was prepared following Baneshi's method with modifications [23]. Carboxylated Fe_3O_4 magnetic beads (1 mg) were washed with PBS for 3 times. The beads were activated with 20 mg EDC and 15 mg NHS in 200 μL of PBS for 1 h. Then 30 μL of 10 μM NH_2-Apt in pH 8.0 Tris-EDTA buffer (Tris-HCl of 10 mmol/L, EDTA of 1 mmol/L) was added. Then it was incubated with shaking for 1 h and wash three times with PBS through magnetic separation. The Apt-Fe_3O_4 magnetic beads was resuspended in pH 7.4 0.01 M PBS buffer (5 mmol/L $MgCl_2$, 1 mmol/L $CaCl_2$).

2.5. Bacterial cultivation

The bacterial strains were cultured under anaerobic conditions in MRS broth medium at 37 ℃ for 10-12 h until reaching the logarithmic growth phase. Bacterial cells were harvested by centrifugation, resuspended in sterile PBS, and serially diluted tenfold. The standard plate counting method was used to analyze the bacteria content.

2.6. Detection of B. bifidum by the sandwich SERS detection system

For liquid-type sample, 1 mL of sample was added into 9 mL sterilized PBS. It was further centrifuged at 3000 r/min for 5 min to remove the white aggregates on top, and then resuspended to 10 mL. For solid-type sample, 1g sample was added 9 mL sterilized PBS for homogenization. Then similar treatment was conducted as the liquid-type sample. For detection, 1 mL of the obtained sample solution was incubated with Apt-Fe_3O_4 probe at 37 ℃. After incubation, magnetic separation was conducted and the particles were washed with PBS for 3 times. Apt-AuNPs@MIL-101 was mixed with the complex to allow incubation. Following the magnetic

washing, SERS measurements was conducted by the portable Raman spectrometer (785 nm excitation wavelength, 1000 ms integration time, and 100 mW laser power).

2.7. Specificity assay

To evaluate specificity, five non-target lactic acid bacteria at ~10^5 CFU/mL were tested along with *B. bifidum*.

2.8. Spiked sample test

To evaluate the reliability of the method, spiked samples (2×10^3, 2×10^4, and 2×10^5 CFU/mL) were prepared by adding *B. bifidum* to 1 mL filtered milk. The samples were shaken to evenly distribute the bacteria. The samples were then added in 9 mL sterile PBS and centrifuged at 3000 r/min for 5 min to remove lipids. Followed by adjusting the volume and shaking to mix uniformly, the *B. bifidum* was analyzed as the method in Section 2.6 and recoveries were calculated.

2.9. Commercial sample analysis

The developed sandwich-type SERS assay was applied to detect *B. bifidum* in commercially products. Results were validated against qPCR to confirm the method's practical applicability.

3. Results and Discussion

3.1 Detection Principle

A sandwich-type SERS aptasensor was developed for *B. bifidum* using Apt-Fe_3O_4 magnetic beads as the capture probe and Apt-AuNPs@MIL-101 as the signal enhancement probe (Scheme 1). NH_2-Apt was covalently grafted onto the surface of Fe_3O_4 magnetic beads, serving as specific capture probe for *B. bifidum*. AuNPs@MIL-101 was synthesized via an *in-situ* AuNP growth on MIL-101 (Cr), which was further functionalized with SH-Apt to form the signal enhancement probe Apt-AuNPs@MIL-101. In the presence of target bacteria, the magnetic capture probe selectively bound the bacteria, which was then combined with the signal enhancement probe Apt-AuNPs@MIL-101 to form a sandwich structure. The *B. bifidum* could then be identified by the characteristic fingerprint patterns in the obtained Raman spectra and be quantified by SERS signal intensity.

3.2 Fabrication of the Apt-AuNPs@MIL-101 signal enhancement probe

The AuNPs@MIL-101 was firstly prepared by the *in-situ* growth method. As Fig. 1A shows, the AuNPs@MIL-101 exhibited a distinctive characteristic absorption peak of the AuNPs at approximately 550 nm, which was absent in MIL-101 (Cr). Moreover, the XRD results demonstrated the emergence of new (111) and (200) lattice planes in AuNPs@MIL-101 (Fig. 1B), yet not in MIL-101 (Cr), further suggesting the formation of the AuNPs. The TEM and SEM images show the preserved octahedral structure of the MIL-101 (Cr), with AuNPs visibly and evenly distributed on the AuNPs@MIL-101 (Fig. 1C). Moreover, there was little difference in the FT-IR spectra of the MIL-101 and AuNPs@MIL-101 (Fig. 1D). According to the EDS and EDX results (Fig. S1 and S2), the contents of the Au element increased significantly after AuNP

formation on the MIL-101 (Cr) and evenly distributed AuNPs could be oberved. Moreover, the XPS spectra (Fig. 1E and F) showed that the AuNPs@MIL-101 presented with an extra Au 4f peak in comparison to the MIL-101 (Cr), indicating the presence of the Au elements on the composites. Fig. 1F and Fig. S3 shows the specific XPS spectra of the Au 4f peaks, indicating that Au was present in the composite particles in different valence states [24,25]. Also, the hydrodynamic size increased from 280.53 ± 5.80 nm to 285.23 ± 7.12 nm for the MIL-101 (Cr) and AuNPs@MIL-101, due to the formation of the AuNPs (Fig. 1H). The zeta potential of the MIL-101 (Cr) and AuNPs@MIL-101 were 31.43 ± 1.07 mV and -20.40 ± 0.10 mV, respectively, indicating the negatively charged AuNPs were formed on the positively charged MIL-101 (Cr) for the AuNPs@MIL-101 group (Fig. 1G). These results illustrated the successful synthesis of the AuNPs@MIL-101.

The SH-Apt was modified on the surface of AuNPs@MIL-101. The characteristic peaks of O-C-O vibration at 948 cm^{-1} of ribose and P-O-C vibration of phospholipid bond at 1020 cm^{-1} of Apt were observed (Fig. 1D) for the Apt-AuNPs@MIL-101 [26–29], indicating the successful modification of the Apt. Moreover, the hydrodynamic size (Fig. 1H) increased from 285.23 ± 7.12 nm for the AuNPs@MIL-101 to 302.33 ± 3.68 nm for the Apt-AuNPs@MIL-101. The average zeta potential of the AuNPs@MIL-101 and Apt-AuNPs@MIL-101 were -20.40 ± 0.10 mV and -30.10 ± 0.45 mV (Fig. 1G), further indicating the modification of the Apt.

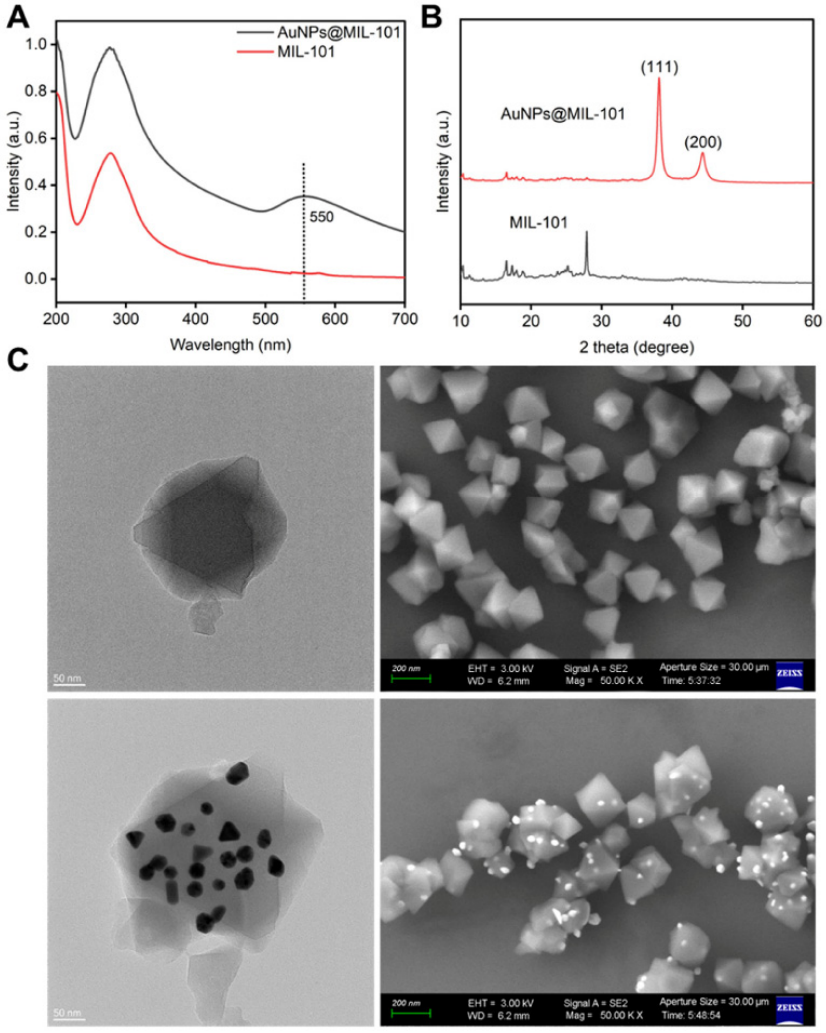

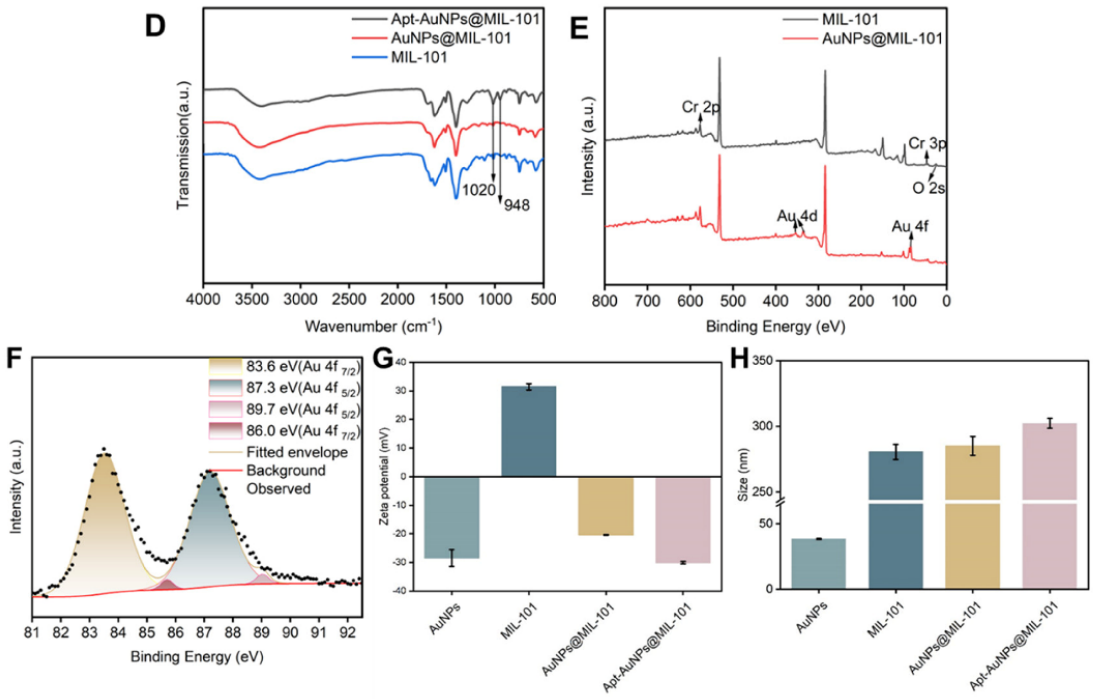

Fig. 1. Preparation of the Apt-AuNPs@MIL-101 signal enhancement probe. (A) UV-Vis absorption spectra. (B) XRD patterns of the MIL-101 (black) and AuNPs@MIL-101 (red). (C) TEM and SEM images of the MIL-101 (upper row) and AuNPs@MIL-101 (lower row). Scale bar for TEM: 50 nm; Scale bar for SEM: 200 nm. (D) FT-IR spectra. (E) XPS of the MIL-101 and the AuNPs@MIL-101. (F) XPS spectra of the Au 4f. (G) Zeta potential analysis and (H) hydrodynamic size analysis.

The Raman signal enhancement ability of the substrates was evaluated using classical 4-mercaptobenzoic acid (4-MBA) as a signaling molecule. Based on the SERS intensity of 4-MBA at 1075 cm^{-1} (Fig. 2A and B), it can be seen that for 4-MBA alone the signal was low. The SERS signal of 4-MBA was significantly enhanced with the enhancement effect of AuNPs@MIL-101, which indicated that it had excellent signal amplification ability. In addition, the 4-MBA signal enhanced by the AuNPs@MIL-101 was distinctly higher than that of the AuNPs and the MIL-101 (Cr) MOF. The high SERS enhancement capability of the AuNPs@MIL-101 substrate was mainly attributed to the uniformly distributed AuNPs on the MIL-101 (Cr), which allowed the formation of homogeneously distributed hot spots [30]. Notably, the signal enhancement ability of the Apt-AuNPs@MIL-101 probe was a little bit lower than the AuNPs@MIL-101 substrate. But overall, Apt-AuNPs@MIL-101 possessed excellent SERS enhancement ability. The relative standard deviation (RSD) analysis of the samples with 0.1 mmol/L or 0.01 mmol/L 4-MBA was performed under the enhancement of Apt-AuNPs@MIL-101 (Fig. S4). The RSD was 5.1% at 0.1 mmol/L and 3.0% at 0.01 mmol/L, indicating the good precision for SERS analysis.

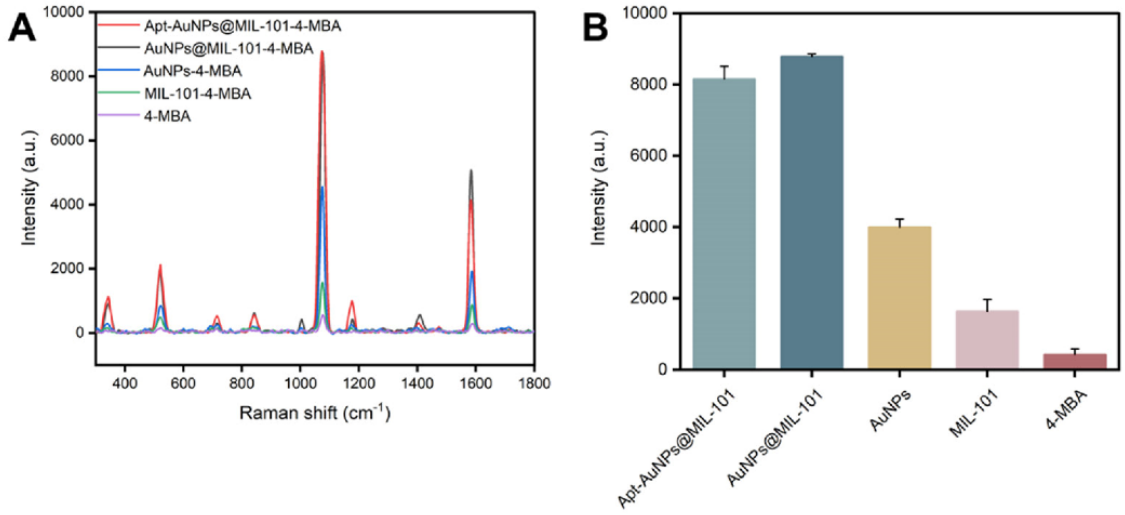

Fig. 2. Analysis of the Raman enhancement capability. (A) Raman spectra and (B) intensities at 1075 cm^{-1}.

3.3 Fabrication of the Apt-Fe3O4 capture probe

The surface of the spherical Fe_3O_4 magnetic beads (Fig. 3A) was modified with the Apt to prepare the Apt-Fe_3O_4 capture probe. As Figure 3B shows, the Apt-Fe_3O_4 showed a characteristic absorption peak of Apt at 260 nm in the UV-Vis spectra, indicating the successful conjugation of the Apt on the magnetic bead. Figure 3C further shows the FT-IR spectra of the Fe_3O_4 magnetic bead and the Apt-Fe_3O_4 magnetic bead. The Fe_3O_4 magnetic beads exhibited Fe-O peaks at 475 cm^{-1} and 586 cm^{-1}, as well as carboxyl groups at 1634 cm^{-1} and 3421 cm^{-1} [31]. In comparison, the Apt-Fe_3O_4 magnetic beads exhibited peaks at 3320 cm^{-1} and 1590 cm^{-1} attributed to the bending and stretching vibrations of the N-H bonds [32,33], indicating that the Apt was successfully modified on the surface of the beads. Meanwhile, the hydrodynamic size (Fig. 3D) increased from 208.33 ± 7.31 nm for Fe_3O_4 beads to 218.04 ± 2.05 nm. The zeta potential (Fig. 3E) of the negatively charged Fe_3O_4 beads (-17.50 ± 1.05 mV) become -22.33 ± 0.95 mV after grafting of the Apt, which further indicated the successful modification of the Apt. Due to the Apt modification, the magnetic properties of Apt-Fe_3O_4 magnetic beads were weakened compared with Fe_3O_4 magnetic beads (Fig. 3F). These results indicated that the Apt was successfully grafted on the surface of the magnetic beads.

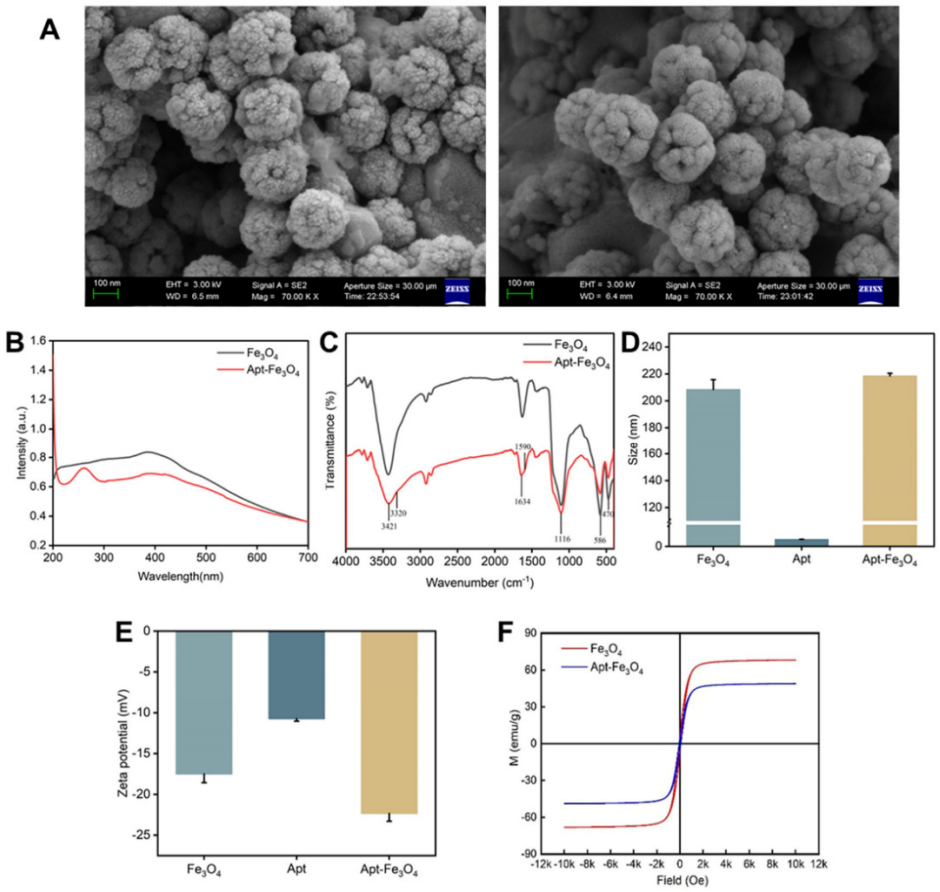

Fig. 3. Preparation of the Apt-Fe_3O_4 capture probe. (A) SEM images of the Fe_3O_4 magnetic bead (left column) and Apt-Fe_3O_4 magnetic bead (right column). Scale bar: 100 nm. (B) UV-Vis absorption spectra of the Apt-Fe_3O_4 magnetic bead (red) and Fe_3O_4 magnetic bead (black). (C) FT-IR spectra of the Apt-Fe_3O_4 magnetic bead (red) and Fe_3O_4 magnetic bead (black). (D) Hydrodynamic size analysis. (E) Zeta potential analysis. (F) Hysteresis regression curve of the Fe_3O_4 magnetic bead (red) and Apt-Fe_3O_4 magnetic bead (blue).

3.4 Optimization of the detection conditions

For *B. bifidum* detection, it was firstly captured by the Apt-Fe_3O_4 capture probe, and then interacted with the signal enhancement probe Apt-AuNPs@MIL-101 to form the sandwich structures for detection (Scheme 1). In this process, factors such as the content of the magnetic capture probe, the capture time, the content of the signal enhancement probe, and the incubation time of the enhancement probe with the capture probe-target bacteria complex were of significant importance for the quantitative detection of *B. bifidum*. The peak intensity of *B. bifidum* at 730 cm^{-1} was employed as an indicator to optimize these conditions. The optimization of the capture probe contents (Fig. S5) revealed that when the content of the capture probe was in the range of 0.5 mg-1.5 mg, the SERS signal of *B. bifidum* gradually increased with the increased content of the capture probe, as the enhanced probe content may enhance the amount of captured target strain, resulting in enhanced SERS signal. When the probe content was 1.5 mg, the SERS intensity was strongest, and after 1.5 mg, the SERS signal began to weaken, which may be due to the probe aggregation that weakened the signal. Therefore, 1.5 mg of capture probe was selected for subsequent experiments. The capture time was then optimized (Fig. S6). When the capture time was increased from 10 min to 40 min, the SERS signal intensity of the target bacteria gradually increased and tended to be stable. When the capture time was longer than 40 min, the SERS signal gradually decreased, which may be due to the reason that Apt-Fe_3O_4 became relatively

unstable in the bacterial solution when the capture time was too long. Consequently, the capture time of 40 min was selected for subsequent experiments. The content of signal enhancement probes (Fig. S7) was also optimized. When the content of the signal enhancement probe increased from 0.1 mg to 0.3 mg, the SERS signal of the target bacteria gradually increased, and when its content was 0.3 mg, the SERS intensity of the target strain was the strongest. When the content surpassed 0.3 mg, the signal intensity of the target strain decreased with the increase of the probe content, which may be because the excessive content would hamper the stability of probes and affected the detection of *B. bifidum*. Therefore, the 0.3 mg substrate was selected for subsequent experiments. Finally, the incubation time of the enhancement probe with the capture probe-target bacteria complex was optimized (Fig. S8). According to the results, when the incubation time was 10-30 min, the SERS intensity gradually increased, reaching the maximum value at 30 min. After more than 30 min, the SERS signal gradually decreased with the extension of time, which may be due to the decreased stability of the complex with the excessive incubation time, resulting in the decrease of SERS signal. Therefore, an optimized incubation time of 30 min was selected.

3.5 Establishment of the detection system

In the detection of *B. bifidum*, distinct signal enhancements were observed at Raman shifts such as 650, 730, 950, 1240, 1325, and 1450 cm^{-1} as *B. bifidum* concentrations increased (Fig. 4A). Preliminary assignments of the vibrational modes are summarized in Table S1. Moreover, the characteristic peaks at 650 cm^{-1} (C-S stretching in tyrosine), 850 cm^{-1} (C-C stretching in the proline ring), and 1080 cm^{-1} (C-O-C stretching of phospholipids) were reported to be the characteristic features that distinguished *B. bifidum* from the widely employed probiotic *Lactobacillus* [34]. Therefore, this fingerprint characteristic from these peaks can be used as indicators for identification of *B. bifidum.*

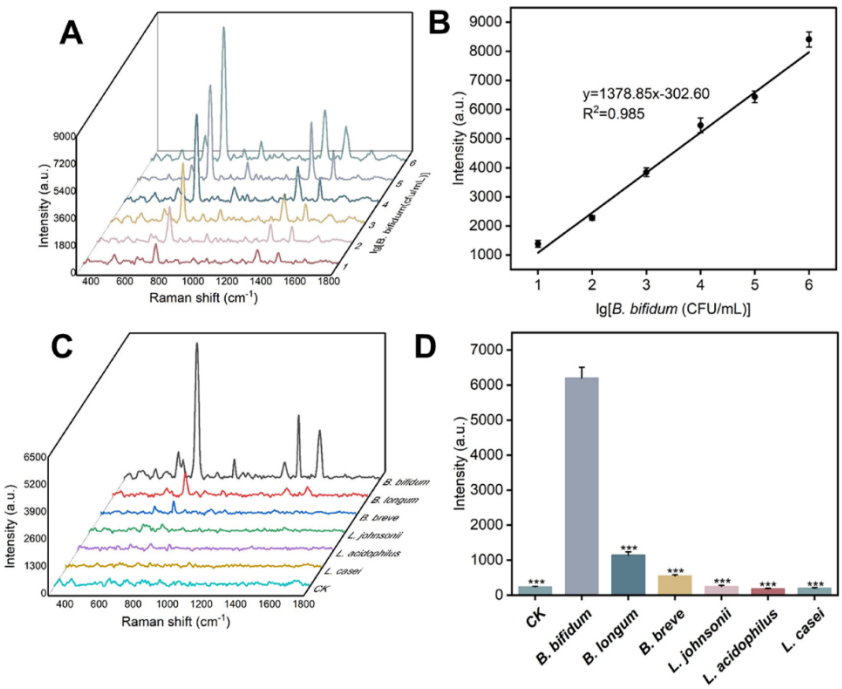

Fig. 4. SERS detection of the *B. bifidum*. (A) Raman plots of *B. bifidum* in the concentration range of 2.0×10^1-2.0×10^6 CFU/mL. (B) Standard curve for SERS detection of the *B. bifidum.* (C) Specificity analysis. (D) Intensity of the peak at 730 cm^{-1} of specificity analysis. *** indicates $P < 0.001$, *t* test.

The Raman peak at 730 cm^{-1}, assigned to adenine vibrational modes, exhibited the most pronounced intensity amplification with increasing bacteria content. Therefore, it was employed as a quantitative indicator for *B. bifidum* analysis. Under the optimized conditions, the SERS response at 730 cm^{-1} exhibited a linear relationship (y=1378.85x–302.60, R^2=0.985) with the logarithmic value of *B. bifidum* concentration at the range of 2.0×10^1-2.0×10^6 CFU/mL (Fig. 4A and 4B). The limit of detection (LOD) of the detection method was determined to be 2.5 CFU/mL (S/N = 3). The sandwich-type SERS assay system in this study was compared with the previous studies for lactic acid bacteria detection (Table 1). It showed ultrasensitive performance than the previous study, highlighting the capability for trace-level quantification of *B. bifidum*. Moreover, the specificity of the method was evaluated using five non-target lactic acid bacteria such as *B. longum*, *B. breve*, *L. johnsonii*, *L. acidophilus*, and *L. casei*. As Figure 4C and 4D shows, the method showed high selectivity towards *B. bifidum*, which could be attributed to the specificy of the Apt.

Table 1 Comparison of various methods for detecting probiotics

Methods	Qualitative or quantitative	LOD (CFU/mL)	Time	Ref
qPCR	Quantitative	10^3	3 h	[35]
Loop-mediated isothermal amplification	Qualitative	10^2	45 min	[36]
16S rRNA gene targeted PCR	Quantitative	10^5	4-6 h	[37]
Propidium monoazide (PMA)-qPCR	Quantitative	/	3 h	[38]
Flow cytometry	Quantitative	10^3	2 h	[39]
ATP-bioluminescence	Quantitative	10^3	30 min	[40]
SERS	Quantitative	2.5	1.5 h	This work

3.6 Application in commercial sample

In order to study the application and reliability of the detection system in actual samples, the following experiments were conducted. The specific detection capability of the detection system for *B. bifidum* in a multi-strain solution was first verified, in which the concentration of *B. bifidum* was fixed at 5×10^7 CFU/mL. The test results are shown in Fig. 5 A and B. A is the control group with *B. bifidum* alone. For Group B, *B. bifidum* and *L. casei*, *B. longum*, *B. breve*, *L. johnsonii*, and *L. acidophilus* were added in a ratio of 1:1:1:1:1:1 (Fig. 5A), while keeping the concentration of *B. bifidum* unchanged. The concentration of non-target strains gradually increased to a ratio of 1:2:2:2:2:2 (C in Fig. 5A), 1:3:3:3:3:3 (D in Fig. 5A), 1:4:4:4:4:4 (E in Fig. 5A), and 1:5:5:5:5:5 (F in Fig. 5A). The results showed that the obtained Raman spectra of *B. bifidum* showed none of the obvious differences from the control group, indicating that the method achieved specific detection of *B. bifidum* in multiple strain samples. In order to verify the stability of the method in the actual sample, we performed a spiked experiment to verify the reliability of the method (Fig. S9 and Table S2). The results showed that the method had good accuracy.

Six commercial probiotic products were selected for application potential analysis. According to the component list, Milk drinks A, Baking powder A, Baking powder B, and Baking powder C were claimed to contain *B. bifidum*, while Baking powder D and pure milk did not contain *B. bifidum*. Under the pretreatment conditions of ten-fold dilution and centrifugal defatting, the SERS analysis was conducted (Figure 5C and

5D). It could be found that the method exhibited generally comparable results with those measured by the classical qPCR method (Table 2). Notably, the sample "Baking powder D" was detected to present with low abundance of *B. bifidum*, while none of the target bacteria was detected by the qPCR method. This could be attributed to the high sensitivity of the proposed SERS method, which could be applicated in the detection of the low abundance samples. Overall, the proposed method showed its practical utility in detecting and quantifying *B. bifidum* in complex matrices.

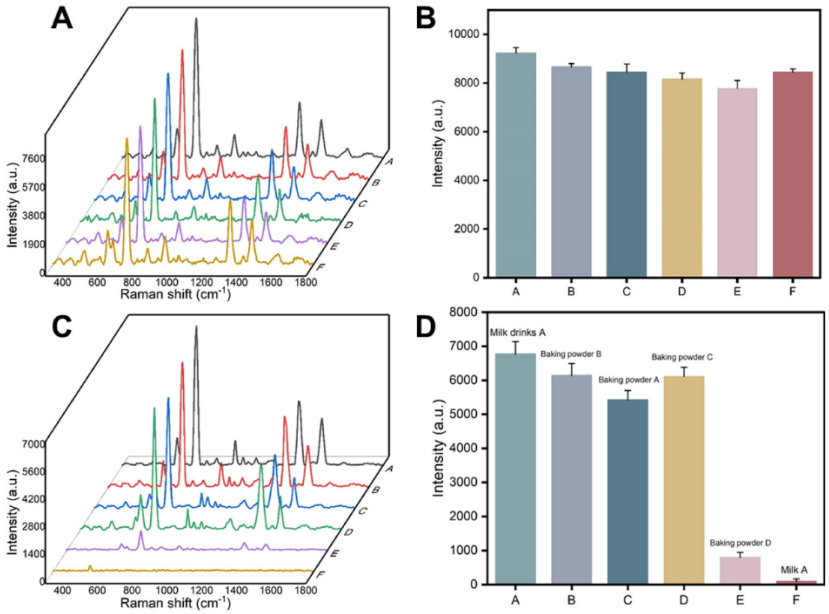

Figure 5. Analysis for multi-strain and commercial samples. (A) Raman plots of *B. bifidum* in multi-strain samples. (B) Raman intensity of the characteristic peaks at 730 cm^{-1}, where A is the control group and B-F are multi-strain samples with different concentrations of non-target bacteria. (C) Raman plots for commercially available products detection. (D) Raman intensity of the characteristic peaks at 730 cm^{-1} for commercially available products detection.

Table 2 Commercial sample analysis

Sample	*B. bifidum* contents detected by the proposed method (Mean ± SD, CFU/mL)	*B. bifidum* contents detected by qPCR (Mean ± SD, CFU/mL)	P
Milk drinks A	$(1.26 \pm 0.87) \times 10^6$	$(5.75 \pm 2.14) \times 10^6$	P=0.2087
Baking powder A	$(1.17 \pm 0.46) \times 10^5$	$(1.89 \pm 1.07) \times 10^5$	P=3365
Baking powder B	$(4.16 \pm 1.97) \times 10^5$	$(6 \pm 2.56) \times 10^5$	P=3709
Baking powder C	$(3.81 \pm 1.83) \times 10^5$	$(3.39 \pm 0.99) \times 10^5$	P=7661
Baking powder D	38 ± 12	ND	/
Milk A	ND	ND	/

SD: standard deviation, n = 3.
$P > 0.05$: no significant difference, t test.

4. Conclusion

This study successfully developed a highly sensitive and specific SERS detection system for *B. bifidum*, based on Apt-Fe_3O_4 capture probe and Apt-AuNPs@MIL-101 signal enhancement probe. The results indicated that the signal intensity obtained by the detection system exhibited a linear relationship with the logarithmic concentration of *B. bifidum*, with the standard curve of y=1378.85x-302.60 (R^2 = 0.985) and LOD of 2.5 CFU/mL. Furthermore, the detection results from commercial products were comparable to those obtained by qPCR, demonstrating the applicability of the method in commercial samples. The sandwich-type

SERS method constructed from Apt-Fe_3O_4 magnetic capture probe and Apt-AuNPs@MIL-101 signal enhancement probe provided a novel approach for the rapid detection of probiotic in complex matrices.

Acknowledgements

This work was supported by the Cross-Innovation Open Project of Food Flavor and Health, Beijing Technology & Business University (No. FFHCI-2025053), National Natural Science Foundation of China (No. 32102079), and Zhejiang Provincial Administration for Market Regulation (ZC2023091).

Reference

[1] Turroni F, Duranti S, Milani C, et al. Bifidobacterium bifidum: a key member of the early human gut microbiota, Microorganisms 7 (2019) 544. https://doi.org/10.3390/microorganisms7110544.

[2] Qi C, Li Z, Tu H, et al. 2'-FL and cross-feeding bifidobacteria reshaped the gut microbiota of infants with atopic dermatitis ex vivo and prevented dermatitis in mice post-microbiota transplantation through retinol metabolism activation, Gut Microbes 17 (2025) 2474148. https://doi.org/10.1080/19490976.2025.2474148.

[3] Zhao J, Zhang G, Yang J, et al. Surface proteins of Bifidobacterium bifidum DNG6 growing in 2′-fucosyllactose alleviating lipopolysaccharide-induced intestinal barrier injury in vitro, J. Dairy Sci. 107 (2024) 8865–8873. https://doi.org/10.3168/jds.2024-25019.

[4] Turroni F, Milani C, Duranti S, et al. The infant gut microbiome as a microbial organ influencing host well-being, Ital. J. Pediatr. 46 (2020) 16. https://doi.org/10.1186/s13052-020-0781-0.

[5] Martín R, Bottacini F, Egan M, et al. The infant-derived bifidobacterium bifidum strain CNCM I-4319 strengthens gut functionality, Microorganisms 8 (2020)1313. https://doi.org/10.3390/microorganisms8091313.

[6] González-González F, Delgado S, Ruiz L, et al. Functional bacterial cultures for dairy applications: Towards improving safety, quality, nutritional and health benefit aspects, Journal of Applied Microbiology 133 (2022) 212–229. https://doi.org/10.1111/jam.15510.

[7] Kamel DG, Hammam ARA, Alsaleem KA, et al. Addition of inulin to probiotic yogurt: viability of probiotic bacteria (*bifidobacterium bifidum*) and sensory characteristics, Food Sci. Nutr. 9 (2021) 1743–1749. https://doi.org/10.1002/fsn3.2154.

[8] Zhang J, Ren L, Zhang L, et al. Single-cell rapid identification, in situ viability and vitality profiling, and genome-based source-tracking for probiotics products, Imeta 2 (2023) e117. https://doi.org/10.1002/imt2.117.

[9] Blaiotta G, De Sena M, De Girolamo F, et al. Probiotic bacilli incorporation in foods: is really so easy? Food Microbiol. 115 (2023) 104342. https://doi.org/10.1016/j.fm.2023.104342.

[10] Peng W, Zhang Y, Yi C, et al. Polyethylene imine-modified photonic crystal microfluidic chip for highly sensitive detection of microbial spores, Food Chem. 459 (2024) 140366. https://doi.org/10.1016/j.foodchem.2024.140366.

[11] Fan X, Li X, Zhang T, et al. A novel qPCR method for the detection of lactic acid bacteria in fermented milk, Foods 10 (2021) 3066. https://doi.org/10.3390/foods10123066.

[12] Hou K, Zhao P, Chen Y, et al. Rapid detection of bifidobacterium bifidum in feces sample by highly sensitive quartz crystal microbalance immunosensor, Front. Chem. 8 (2020) 548. https://doi.org/10.3389/fchem.2020.00548.

[13] Huang Z, Peng J, Xu L, et al. Development and application of surface-enhanced raman scattering (SERS), Nanomaterials 14 (2024) 1417. https://doi.org/10.3390/nano14171417.

[14] Zhang X-L, Zhang H-N, Liang H, et al. Gold nanobipyramid hotspot aggregation-induced surface-enhanced raman scattering for the ultrasensitive detection of miRNA, Anal. Chem. 95 (2023) 12768–12775. https://doi.org/10.1021/acs.analchem.3c01477.

[15] Tian T, Hu X, Huang Y, et al. Enhancing CO_2 photoreduction to CO with 100 % selectivity by constructing heterojunctions and regulating open metal sites in Au/Fe_3O_4/MIL-101(Fe) catalysts, J. Colloid Interface Sci. 680 (2025) 33–41. https://doi.org/10.1016/j.jcis.2024.10.182.

[16] Li Y-F, Zou C-J, Liu X-B, et al. Highly Sensitive and Selective Detection of Pharmaceuticals on Au/MIL-101(Cr) by SERS, Anal. Chem. 95 (2023) 7933–7940. https://doi.org/10.1021/acs.analchem.3c00466.

[17] Zhao S-S, Ma C-J, Xu Y, et al. Fabrication of MIL-101(Cr)/silver nanocomposites as SERS substrate for sensitive determination of malachite green and crystal violet in tilapia, Microchim. Acta 190 (2023) 282. https://doi.org/10.1007/s00604-023-05867-z.

[18] Wu X, Gao S, Niu Y, et al. Quantitative analysis of blended corn-olive oil based on raman spectroscopy and one-dimensional convolutional neural network, Food Chem. 385 (2022) 132655. https://doi.org/10.1016/j.foodchem.2022.132655.

[19] Wang H, Su A, Chang J, et al. Current advance of CRISPR/cas-based SERS technology, Sens. Diagn. 2 (2023) 792–805. https://doi.org/10.1039/D2SD00235C.

[20] Wang X, Li W, Dai S, et al. High-throughput, highly sensitive and rapid SERS detection of *escherichia coli* O157:H7 using aptamer-modified Au@macroporous silica magnetic photonic microsphere array, Food Chem. 424 (2023) 136433. https://doi.org/10.1016/j.foodchem.2023.136433.

[21] Hu L, Wang L, Lu W, et al. Selection, characterization and interaction studies of a DNA aptamer for the detection of bifidobacterium bifidum, Int. J. Mol. Sci. 18 (2017) 883. https://doi.org/10.3390/ijms18050883.

[22] Hu Y, Zhou X, Wang L, et al. A liposome-based aptasensor integrated with competitive reaction enabling portable and electrochemical detection of Aβ oligomer, Biosens. Bioelectron. 225 (2023) 115108. https://doi.org/10.1016/j.bios.2023.115108.

[23] Baneshi M, Dadfarnia S, Shabani AMH, et al. A novel theranostic system of AS1411 aptamer-functionalized albumin nanoparticles loaded on iron oxide and gold nanoparticles for doxorubicin delivery, Int. J. Pharm. 564 (2019) 145–152. https://doi.org/10.1016/j.ijpharm.2019.04.025.

[24] Khaletskaya K, Pougin A, Medishetty R, et al. Fabrication of gold/titania photocatalyst for CO_2 reduction based on pyrolytic conversion of the metal–organic framework NH_2-MIL-125(Ti) loaded with gold nanoparticles, Chem. Mater. 27 (2015) 7248–7257. https://doi.org/10.1021/acs.chemmater.5b03017.

[25] Wang P, Wu L, Lu Z, et al. Gecko-inspired nanotentacle surface-enhanced raman spectroscopy substrate for sampling and reliable detection of pesticide residues in fruits and vegetables, Anal. Chem. 89 (2017) 2424–2431. https://doi.org/10.1021/acs.analchem.6b04324.

[26] Wang J, Guo S, Park E, et al. SERS-based aptamer sensing strategy for diabetes biomarker detection, Anal. Chem. 96 (2024) 20082–20089. https://doi.org/10.1021/acs.analchem.4c05036.

[27] Custovic I, Pocholle N, Bourillot E, et al. Infrared nanospectroscopic imaging of DNA molecules on mica surface, Sci. Rep. 12 (2022) 18972. https://doi.org/10.1038/s41598-022-23637-4.

[28] Neumann O, Zhang D, Tam F, et al. Direct optical detection of aptamer conformational changes induced by target molecules, Anal. Chem. 81 (2009) 10002–10006. https://doi.org/10.1021/ac901849k.

[29] Muntean CM, Dina ,Nicoleta E., Tăbăran, Alexandra, et al. Identification of salmonella serovars before and after ultraviolet light irradiation by fourier transform infrared (FT-IR) spectroscopy and chemometrics, Anal. Lett. 54 (2021) 150–172. https://doi.org/10.1080/00032719.2020.1731524.

[30] Hu Y, Liao J, Wang D, et al. Fabrication of gold nanoparticle-embedded metal–organic framework for highly sensitive surface-enhanced raman scattering detection, Anal. Chem. 86 (2014) 3955–3963. https://doi.org/10.1021/ac5002355.

[31] Zhang Y, Zhu L, Ma X, et al. An effective docking-guided strategy for rational tailoring of fluorescent aptamer switches of dimethylindole red analogue, Anal. Chem. 95 (2023) 7076–7081. https://doi.org/10.1021/acs.analchem.3c01194.

[32] Shen YF, Tang J, Nie ZH, et al. Tailoring size and structural distortion of Fe_3O_4 nanoparticles for the purification of contaminated water, Bioresour. Technol. 100 (2009) 4139–4146. https://doi.org/10.1016/j.biortech.2009.04.004.

[33] Wang J, Zheng S, Shao Y, et al. Amino-functionalized Fe_3O_4@SiO_2 core–shell magnetic nanomaterial as a novel adsorbent for aqueous heavy metals removal, J. Colloid Interface Sci. 349 (2010) 293–299. https://doi.org/10.1016/j.jcis.2010.05.010.

[34] Berus SM, Adamczyk-Popławska M, Goździk K, et al. SERS-PLSR analysis of vaginal microflora: towards the spectral library of microorganisms, Int. J. Mol. Sci. 23 (2022) 12576. https://doi.org/10.3390/ijms232012576.

[35] Li F, Liu J, Maldonado-Gómez MX, et al. Highly accurate and sensitive absolute quantification of bacterial strains in human fecal samples, Microbiome 12 (2024) 168. https://doi.org/10.1186/s40168-024-01881-2.

[36] Kim M-J, Shin SW, Kim H-B, et al. Direct loop-mediated isothermal amplification (LAMP) assay for rapid on-site detection of *bifidobacterium longum* subspecies *longum*, *infantis*, and *suis* in probiotic products, Food Chem. 2021;346:128887. https://doi.org/10.1016/j.foodchem.2020.128887.

[37] Kim E, Yang S-M, Lim B, et al. Design of PCR assays to specifically detect and identify 37 lactobacillus species in a single 96 well plate, BMC Microbiol. 20 (2020) 96. https://doi.org/10.1186/s12866-020-01781-z.

[38] Yang Y, Liu Y, Shu Y, et al. Modified PMA-qPCR method for rapid quantification of viable lactobacillus spp. in fermented dairy products, Food Anal. Methods 14 (2021) 1908–1918. https://doi.org/10.1007/s12161-021-02022-3.

[39] Chiron C, Tompkins TA, Burguière P. Flow cytometry: a versatile technology for specific quantification and viability assessment of micro-organisms in multistrain probiotic products, J. Appl. Microbiol. 124 (2018) 572–584. https://doi.org/10.1111/jam.13666.

[40] Wu H, Wu Q, Zhang J, et al. Study on rapid quantitative detection of total bacterial counts by the ATP-bioluminescence and application in probiotic products, Int. J. Food Sci. Technol. 46 (2011) 921–929. https://doi.org/10.1111/j.1365-2621.2010.02531.x.